

MedAD-R1: Eliciting Consistent Reasoning in Interpretable Medical Anomaly Detection via Consistency-Reinforced Policy Optimization

Haitao Zhang^{1*}, Yingying Wang^{1,2,*}, Jiaxiang Wang^{1,2}, Haote Xu^{3,4}, Hongyang Zhang⁵, Yirong Chen⁶, Yue Huang^{1,2}, Xinghao Ding^{1,2†}

¹School of Informatics, Xiamen University

²Institute of Artificial Intelligence, Xiamen University

³Zhejiang Expressway Co., Ltd.

⁴School of Transportation Science and Engineering, Beihang University

⁵School of Science and Engineering, Chinese University of Hong Kong

⁶Shanghai Artificial Intelligence Laboratory

{haitaozhang0829, wangyingying7, wangjiaxiang}@stu.xmu.edu.cn, hotxu2025@163.com, hongyangzhang1@link.cuhk.edu.cn, Chenyirong@pjlab.org.cn, {yhuang2010, dxh}@xmu.edu.cn

Abstract

Medical Anomaly Detection (MedAD) presents a significant opportunity to enhance diagnostic accuracy using Large Multimodal Models (LMMs) to interpret and answer questions based on medical images. However, the reliance on Supervised Fine-Tuning (SFT) on simplistic and fragmented datasets has hindered the development of models capable of plausible reasoning and robust multimodal generalization. To overcome this, we introduce MedAD-38K, the first large-scale, multimodal, and multi-center benchmark for MedAD featuring diagnostic Chain-of-Thought (CoT) annotations alongside structured Visual Question-Answering (VQA) pairs. On this foundation, we propose a two-stage training framework. The first stage, Cognitive Injection, uses SFT to instill foundational medical knowledge and align the model with a structured think-then-answer paradigm. Given that standard policy optimization can produce reasoning that is disconnected from the final answer, the second stage incorporates Consistency Group Relative Policy Optimization (Con-GRPO). This novel algorithm incorporates a crucial consistency reward to ensure the generated reasoning process is relevant and logically coherent with the final diagnosis. Our proposed model, MedAD-R1, achieves state-of-the-art (SOTA) performance on the MedAD-38K benchmark, outperforming strong baselines by more than 10%. This superior performance stems from its ability to generate transparent and logically consistent reasoning pathways, offering a promising approach to enhancing the trustworthiness and interpretability of AI for clinical decision support.

*Equal contribution.

†Corresponding author.

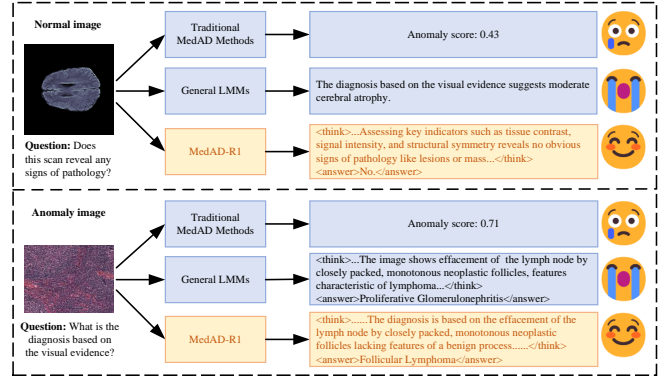


Figure 1: Comparison of MedAD-R1 against traditional methods and general-purpose LMMs. Traditional methods yield uninterpretable anomaly scores, while general models can fail or produce diagnoses inconsistent with their reasoning. MedAD-R1 provides a transparent and logically coherent diagnostic process, enhancing both interpretability and clinical reliability.

1 Introduction

Medical Anomaly Detection (MedAD) plays a vital role in identifying anomalies that may indicate rare diseases or pathological conditions in the clinical diagnostic process. However, the application of Large Multimodal Models (LMMs) to this task is constrained by two core challenges: data scarcity and profound reasoning deficiencies. First, the research landscape is fragmented, lacking unified, large-scale, and multi-center benchmarks required to train and fairly evaluate models for robust generalization [Prevedello *et al.*, 2019]. Existing datasets are often restricted to simple image-level labels, which are insufficient to cultivate sophisticated diagnostic reasoning. Second, and more critically, even models capable of generating explanatory text often fail to produce a trustworthy reasoning process. They may produce fluent diagnostic “thoughts” that are not logically aligned with their final “answer,” reflecting a critical inconsistency

that is unacceptable in high-stakes clinical scenarios and impedes real-world adoption. This distinction is illustrated in Figure 1, where conventional methods offer uninterpretable scores and general LMMs provide incorrect or inconsistent diagnoses, in stark contrast to our model, which delivers a transparent, accurate, and logically coherent diagnostic reasoning process.

Concurrently, the rise of powerful LMMs like LLaVA-Med [Li *et al.*, 2023] and HuatuoGPT-Vision [Chen *et al.*, 2024] has advanced medical image understanding. However, these models are not tailored for MedAD and are hindered by their reliance on a Supervised Fine-Tuning (SFT) paradigm. This training objective primarily teaches models to correlate image-text pairs, incentivizing them to recite learned statistical patterns rather than construct a verifiable, step-by-step causal argument [Gudibande *et al.*, 2023]. This creates a significant risk, as a clinically sound diagnosis requires a verifiably correct reasoning process, not just a correct final answer. This fundamental weakness compromises their reliability, as the lack of an explicit mechanism to enforce logical coherence makes their reasoning untrustworthy. Therefore, there is a clear need for a new framework that moves beyond superficial imitation and instills a deep, consistent reasoning capability in LMMs for MedAD. This requires a paradigm that not only teaches the model domain-specific knowledge but also can explicitly optimize for the logical integrity of its reasoning process.

To systematically address these challenges, we present a comprehensive, three-part research effort. Our first step is to build the necessary foundation: we construct **MedAD-38K**, the first large-scale, multi-modal, and multi-center benchmark for MedAD, uniquely enriched with the structured VQA pairs and Chain-of-Thought (CoT) annotations required to train and evaluate sophisticated reasoning. These CoT annotations provide the explicit, step-by-step supervisory signal necessary to teach a model how to reason, rather than merely generating the answer. With this benchmark in place, our second step was to develop a novel training framework, culminating in our model, **MedAD-R1**. We propose a two-stage paradigm that begins with a Cognitive Injection stage (SFT) to instill foundational medical knowledge, followed by a Reasoning Reinforcement stage (RL) featuring our novel algorithm, **Consistency Group Relative Policy Optimization (Con-GRPO)**. Con-GRPO is specifically designed to overcome the reasoning-answer disconnect by incorporating a crucial consistency reward, explicitly compelling the model’s thought process to logically support its final diagnosis. As our final step, we use a held-out portion of our dataset to establish a rigorous benchmark where MedAD-R1 demonstrates state-of-the-art (SOTA) performance, outperforming a wide range of strong baselines. Notably, this superior performance is achieved with a lightweight 3B parameter model, underscoring its potential for efficient, practical deployment in resource-constrained clinical environments.

Our contributions are summarized as follows:

- We introduce MedAD-38K, the first benchmark for MedAD specifically designed to train and evaluate diagnostic reasoning. Its large-scale, multi-modal, and multi-center composition, enriched with VQA pairs and

CoT annotations, provides a foundational resource for developing more transparent medical AI.

- We propose a novel two-stage training framework, featuring our Con-GRPO algorithm, that enables LMMs to transcend superficial correlations and cultivate deep, consistent reasoning for medical diagnostics.
- Our model, MedAD-R1, significantly outperforms strong baselines on MedAD-38K, achieving up to a 10% absolute improvement in diagnostic accuracy while generating transparent and verifiable reasoning pathways that enhance clinical trustworthiness.

2 Related Work

2.1 Medical Anomaly Detection

Early approaches to Medical Anomaly Detection (MedAD) primarily centered on reconstruction [Cai *et al.*, 2024; Iqbal *et al.*, 2023] or feature-matching paradigms [Zhang *et al.*, 2024]. These methods, often based on Autoencoders or Diffusion Models, learn the data distribution of healthy tissue and identify anomalies as deviations from this norm. While foundational, these traditional methods suffer from several critical limitations that hinder their clinical utility. For instance, they often exhibit poor generalization when faced with new imaging protocols or patient demographics. Furthermore, they lack the capacity for dialogue, operating as static, non-interactive systems. Most critically, they function as black boxes, failing to provide the transparent, step-by-step reasoning that is essential for building clinical trust. Our work directly addresses this final, pivotal limitation.

2.2 Large Multimodal Models in Medicine

The proliferation of Large Multimodal Models (LMMs) has marked a paradigm shift in AI, catalyzing the development of specialized medical LMMs to handle domain-specific data that general-purpose models like GPT-4o [Achiam *et al.*, 2023] often misinterpret. A common architectural blueprint involves a pre-trained vision encoder, a projection module, and a large language model decoder. For instance, LLaVA-Med [Li *et al.*, 2023] continues pre-training on a large corpus of biomedical figure-caption pairs, leveraging a Large Language Model (LLM) to generate VQA instructions from the contextual text. Meanwhile, Med-Flamingo [Moor *et al.*, 2023] adapts the Flamingo VLM by inserting new cross-attention layers for medical tuning. While these models demonstrate impressive capabilities in generating fluent medical descriptions, their reliance on SFT is a critical weakness. The SFT objective incentivizes the learning of superficial mappings between visual features and textual patterns, rather than fostering a true causal reasoning process. This can lead to models that generate plausible-sounding but logically flawed or “hallucinated” explanations. In contrast, our work introduces the first LMM framework designed specifically for MedAD, moving beyond the limitations of SFT by explicitly reinforcing the logical consistency required for a trustworthy diagnostic process.

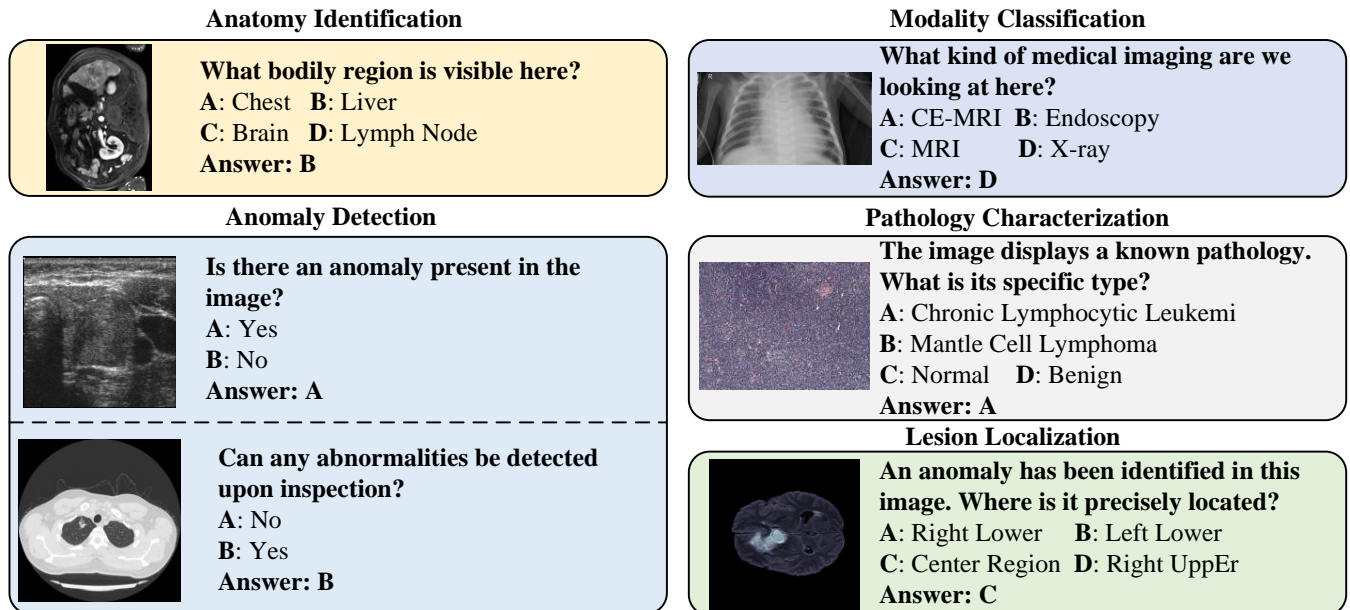


Figure 2: Illustrative examples of the five core VQA tasks within the MedAD-38K benchmark. Each task is structured in a multiple-choice format to facilitate standardized evaluation.

2.3 Reasoning via CoT and RL

CoT prompting has emerged as a powerful technique for improving model interpretability by eliciting intermediate reasoning steps. Recent efforts have extended this paradigm to multimodal contexts, decomposing vision-language tasks into sequential steps [Zhang *et al.*, 2023]. While SOTA foundation models have demonstrated impressive CoT-style reasoning on natural images [Comanici *et al.*, 2025], applying these methods to medical imagery presents distinct challenges. Unlike natural scenes grounded in common-sense semantics, medical diagnosis hinges on complex anatomical principles and subtle pathological cues, lacking the photorealistic, common-sense context of the natural world. Generating a clinically valid reasoning trace requires specialized domain knowledge, not just general visual understanding. To our best knowledge, no prior work has systematically developed a training paradigm to first generate and then explicitly reinforce a verifiable, step-by-step diagnostic reasoning process for MedAD.

3 Methodology

MedAD-R1 is built upon MedAD-38K, a benchmark designed to foster sophisticated reasoning. As the first large-scale MedAD benchmark with detailed CoT annotations, MedAD-38K provides the foundation for our two-stage training paradigm. We first learn a structured reasoning process through SFT on MedAD-38K, and then enforce logical consistency between the reasoning steps and the final diagnosis using our Con-GRPO algorithm. This two-stage approach bridges a critical gap in multimodal explainability for high-stakes medical applications. In this section, we detail the construction of MedAD-38K and the architecture of MedAD-R1.

3.1 The MedAD-38K Benchmark

A primary obstacle to developing robust, reasoning-capable models for MedAD is the lack of a unified, large-scale benchmark. Existing datasets are often fragmented, limited to a single modality or anatomical region, and typically only provide image-label pairs, which are insufficient for training or evaluating the complex, multi-dimensional capabilities of LMMs. To address this critical gap, we construct MedAD-38K, a comprehensive benchmark created by aggregating and re-annotating a wide array of public datasets. This effort involves integrating data from prominent sources such as BraTS2021 [Baid *et al.*, 2021], LiverCT [Bilic *et al.*, 2023], Retinal Edema Segmentation Challenge (RESC) [Hu *et al.*, 2019], BUSI [Al-Dhabayani *et al.*, 2020], ISIC2018 [Codella *et al.*, 2019], Mosmed [Morozov *et al.*, 2020], ATLAS [Al-saheel *et al.*, 2021], DDTI [Pedraza *et al.*, 2015], Kvasir-SEG [Jha *et al.*, 2019], CVC-ClinicDB [Bernal *et al.*, 2015], PH² [Mendonça *et al.*, 2013], IDRiD [Porwal *et al.*, 2018], PediDemi [Popa and Visa, 2025], Br35H [Hamada, 2020], Chest X-ray [Wang *et al.*, 2017], Malignant Lymphoma Classification [Orlov *et al.*, 2010], and BACH [Aresta *et al.*, 2019]. This comprehensive aggregation results in an exceptionally diverse benchmark. It encompasses 10 distinct imaging modalities, including MRI, CT, OCT, Ultrasound, Dermoscopy, CE-MRI, Endoscopy, Fundus, X-ray, and Microscopy. This multi-modal data covers 10 different anatomical regions: Brain, Liver, Retina, Breast, Skin, Lung, Thyroid, Alimentary, Chest, and Lymph Node.

To move beyond simple classification and enable sophisticated model training, we enrich every image in MedAD-38K with a structured VQA task. For each image, we generate a series of questions designed to probe the model’s understanding across five core diagnostic axes: *Anatomy Identifi-*

cation, Modality Classification, Anomaly Detection, Pathology Characterization and Lesion Localization, as illustrated in Figure 2. To enhance model robustness against linguistic variations, each task category includes 10 synonymous but differently phrased questions. For precise and automated evaluation, all questions are formulated in a multiple-choice format with four options. To standardize the output for lesion localization, we define five discrete spatial regions: Left Upper, Right Upper, Left Lower, Right Lower, and Center Region, as depicted in Figure 4.

The cornerstone of MedAD-38K is the integration of diagnostic reasoning pathways, created through the multi-stage pipeline illustrated in the top panel of Figure 3. We generate high-quality CoT annotations using a systematic process. First, for each image, we leverage the MedGemma [Sellergren *et al.*, 2025] model to produce a detailed textual description of its visual content. Next, using predefined templates, we generate a structured VQA pair for each of the five diagnostic axes. This QA pair, along with the image and its description, is then supplied as a prompt to the Gemini 2.5 Pro [Comanici *et al.*, 2025] model to generate an initial CoT. Finally, to guarantee clinical accuracy and logical soundness, every generated CoT undergoes a rigorous manual verification process. Annotations are accepted only if they demonstrated self-consistent reasoning, are grounded in the question, and provided a stepwise justification. Conversely, any outputs containing hallucinated facts, premature conclusions, or circular logic are rejected and refined. This meticulous process ensures that MedAD-38K is a high-quality and challenging resource for training and evaluating reasoning-centric MedAD models.

3.2 The MedAD-R1 Framework

The architecture of our proposed model, MedAD-R1, is designed to process multimodal inputs and generate a structured, two-part output comprising a diagnostic reasoning trace and a final answer. As illustrated in Figure 3, the model takes a medical image I and a corresponding textual question Q as input. It then generates a structured output Y , which consists of a CoT text, denoted as the thought T , and a final diagnostic answer A .

3.3 Cognitive Injection via SFT

The primary goal of the first stage is twofold: (i) to inject the model with foundational, multi-modal medical knowledge from our rich MedAD-38K benchmark, and (ii) to align the model’s output with our desired structured reasoning format, `<think>...</think><answer>...</answer>`. SFT is ideally suited for this purpose, as it efficiently enables the model to internalize the high-quality, expert-curated data we have prepared.

During this stage, we train the model to maximize the likelihood of generating the ground-truth output $Y^* = (T^*, A^*)$ for each sample (I, Q, Y^*) in our dataset $\mathcal{D}_{\text{MedAD-38K}}$. This is achieved by minimizing the negative log-likelihood loss, a standard cross-entropy objective:

$$\mathcal{L}_{\text{SFT}}(\theta) = - \sum_{(I, Q, Y^*) \in \mathcal{D}_{\text{MedAD-38K}}} \log \pi_{\theta}(Y^* | I, Q) \quad (1)$$

This process effectively fine-tunes the general-purpose LMM to understand the specific nuances of medical imagery and terminology, while simultaneously conditioning it to adopt the “think-then-answer” behavioral pattern. The resulting model, denoted as π_{SFT} , serves as a capable baseline and a crucial starting point for the subsequent reinforcement learning phase.

3.4 Reasoning Reinforcement via Con-GRPO

While SFT provides a strong foundation, it encourages the model to learn a superficial mapping from input to output. This may lead to a critical disconnect between the generated reasoning T and the final answer A , undermining the model’s trustworthiness. To address this, we introduce a reinforcement learning (RL) stage to explicitly reward the model for logical consistency.

While standard on-policy algorithms like PPO [Schulman *et al.*, 2017] are effective, they typically rely on a learned value function for advantage estimation. This typically requires an additional neural network of comparable size to the policy model itself. In the context of LMMs, this imposes a substantial memory and computational burden. To circumvent this, we build our method upon Group Relative Policy Optimization (GRPO) [Shao *et al.*, 2024], a memory-efficient variant of PPO. GRPO obviates the need for a value function by instead using the average reward of a group of sampled outputs as a dynamic baseline.

Our algorithm, Con-GRPO, adapts this efficient framework and enhances it with a novel reward function tailored for diagnostic reasoning. The overall objective is to fine-tune the SFT policy π_{SFT} into a new policy π_{θ} that maximizes the expected reward:

$$J(\theta) = \mathbb{E}_{(I, Q) \sim \mathcal{D}, Y \sim \pi_{\theta}(\cdot | I, Q)} [R(Y)] \quad (2)$$

where $R(Y)$ is our custom reward function.

Reward Function Design

The core of Con-GRPO lies in its reward function, which is a composite signal designed to incentivize three key aspects of the model’s output: structural correctness, accuracy, and logical coherence. In the high-stakes context of MedAD, we posit that an output is only valuable if it is simultaneously well-structured, correct, and internally consistent. A failure in any one of these aspects renders the entire generation clinically untrustworthy. We therefore treat all three components as equally important, as any output that does not meet all criteria is considered fundamentally flawed. A simple format reward, R_{fmt} , provides a binary signal to ensure the output adheres to the required `<think>...</think><answer>...</answer>` structure. The total reward is formulated as an equal-weighted sum of a format reward, an accuracy reward, and our proposed consistency reward:

$$R(Y) = \lambda_{\text{fmt}} R_{\text{fmt}}(Y) + \lambda_{\text{acc}} R_{\text{acc}}(A, A^*) + \lambda_{\text{con}} R_{\text{con}}(T, A, Q) \quad (3)$$

where we set the scalar weights equally, $\lambda_{\text{fmt}} = \lambda_{\text{acc}} = \lambda_{\text{con}} = 1/3$, to enforce this equal priority.

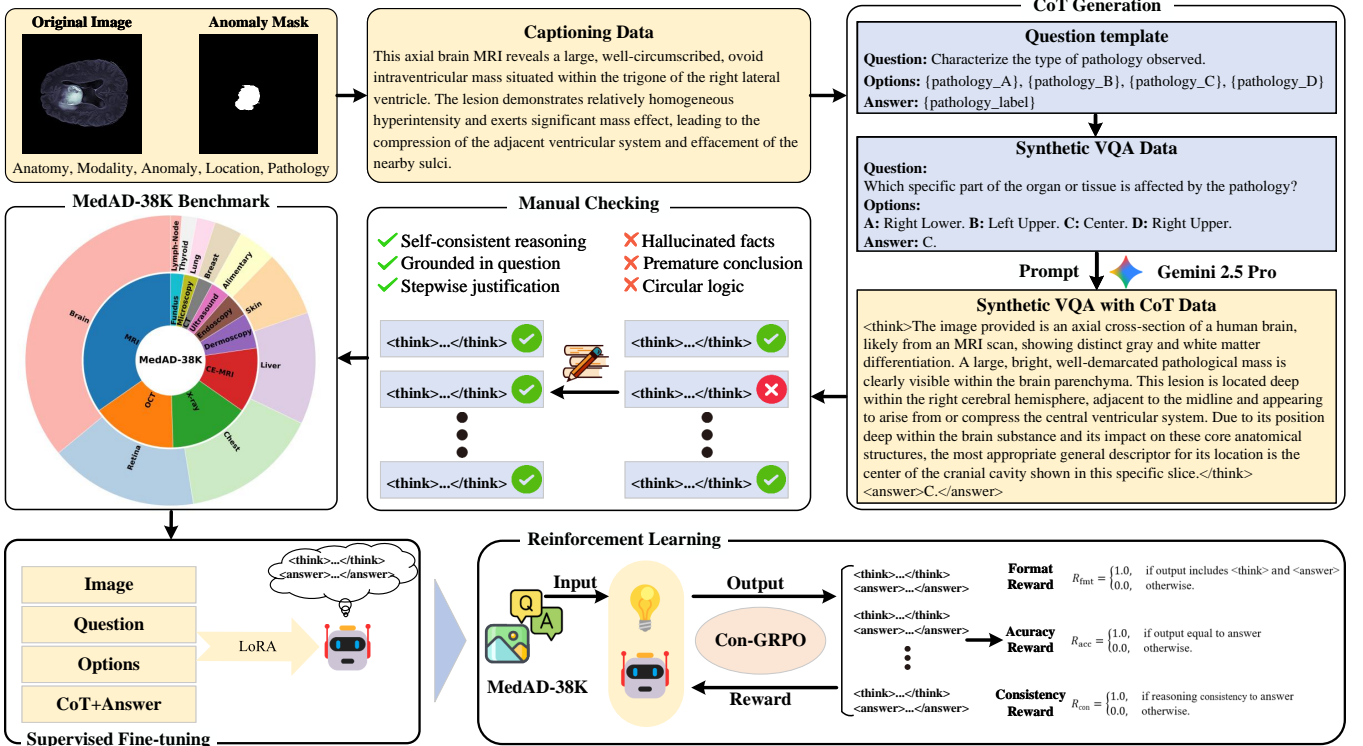


Figure 3: An overview of our entire pipeline. **Top:** The construction process for the MedAD-38K benchmark, detailing the automated CoT generation using large models followed by a rigorous manual verification phase. **Bottom:** The two-stage training architecture of MedAD-R1, which starts with Supervised Fine-tuning to align the model, followed by our Con-GRPO algorithm to reinforce logical reasoning.

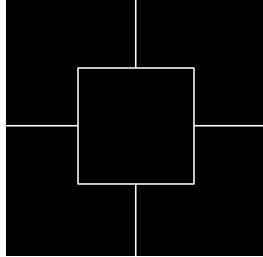


Figure 4: The five-region spatial grid used for lesion localization in the MedAD-38K benchmark.

The Format Reward (R_{fmt}) strictly enforces structural adherence. It is defined as:

$$R_{\text{fmt}} = \begin{cases} 1.0, & \text{if } Y \text{ contains properly enclosed} \\ & \quad \text{tags } <\text{think}> \text{ and } <\text{answer}> \\ 0.0, & \text{otherwise.} \end{cases} \quad (4)$$

The Accuracy Reward (R_{acc}) evaluates the correctness of the final prediction, defined as:

$$R_{\text{acc}}(A, A^*) = \mathbb{I}(A = A^*) \quad (5)$$

The Consistency Reward (R_{con}) constitutes our key innovation. It ensures the logical coherence between the thought process T and the final answer A . We use an external LMM as an evaluator \mathcal{F} to deduce an answer based solely on the

generated thought process. The reward is 1 if and only if this deduced answer matches the model's own generated answer:

$$R_{\text{con}}(T, A, Q) = \mathbb{I}(\mathcal{F}(T, Q) = A) \quad (6)$$

This holistic reward mechanism effectively penalizes deviations from the desired format, correctness, or internal consistency, establishing a rigorous foundation for trustworthy medical diagnostics.

Policy Optimization with Con-GRPO

Adopting the GRPO framework, for each input (I, Q) , we sample a group of G outputs $\{Y_1, \dots, Y_G\}$ from our current policy π_θ . We then calculate the Group-Relative Advantage for each output Y_i by comparing its total reward $R(Y_i)$ against the average reward of the group, which serves as the baseline:

$$\hat{A}(Y_i) = R(Y_i) - \frac{1}{G} \sum_{j=1}^G R(Y_j) \quad (7)$$

This advantage estimate, $\hat{A}(Y_i)$, is then used in the policy update. Let $r_t(\theta)$ be the probability ratio for a token y_t in an output sequence Y : $r_t(\theta) = \frac{\pi_\theta(y_t | I, Q, y_{<t})}{\pi_{\text{SFT}}(y_t | I, Q, y_{<t})}$. The final optimization objective for Con-GRPO is to maximize:

$$\begin{aligned} \mathcal{L}_{\text{Con-GRPO}}(\theta) = \mathbb{E} \left[\sum_t \min \left(r_t(\theta) \hat{A}_t, \text{clip}(r_t(\theta), 1 - \epsilon, 1 + \epsilon) \hat{A}_t \right) \right. \\ \left. - \beta D_{\text{KL}}(\pi_\theta(\cdot | I, Q) || \pi_{\text{SFT}}(\cdot | I, Q)) \right] \end{aligned} \quad (8)$$

where ϵ is the clipping hyperparameter and β controls the KL-divergence penalty preventing deviation from the SFT policy. By leveraging the memory efficiency of GRPO’s baseline and the logical grounding of our consistency reward, Con-GRPO provides a robust solution for training large, reliable, and interpretable models tailored to the high-stakes domain of MedAD.

4 Experiments

In this section, we conduct a series of experiments to rigorously evaluate the performance of our proposed model, MedAD-R1. We aim to answer two primary questions: (1) Does MedAD-R1 outperform SOTA medical and general-purpose LMMs on our challenging benchmark? (2) How effective is our two-stage training paradigm in improving diagnostic accuracy and reasoning?

4.1 Experimental Setup

Dataset and Evaluation Metrics. We evaluate all models on the test set of our newly constructed MedAD-38K benchmark, which comprises 30% of the total dataset. Our primary evaluation metric is Accuracy, which we calculate for each of the five core diagnostic tasks (Anatomy Identification, Anomaly Detection, Lesion Localization Modality Classification and Pathology Characterization). The task-specific accuracy is the ratio of correctly answered questions to the total number of questions for that task. Finally, we report the Overall Accuracy, calculated as the total number of correct answers across all tasks in the test set divided by the total number of questions.

Implementation Details. Our proposed method, MedAD-R1, is built upon the Qwen2.5-VL-3B [Bai *et al.*, 2025] backbone. All experiments are implemented in PyTorch using the AdamW [Kingma and Ba, 2014] optimizer with bfloat16 precision and a global batch size of 64. For Stage 1 (SFT), we employ LoRA and train for 2 epochs with a learning rate of 1.0×10^{-4} . For Stage 2 (Con-GRPO), we train for a single epoch with a lower learning rate of 1.0×10^{-6} to stabilize the reinforcement learning process. Key hyperparameters for Con-GRPO include a group size G of 8 and a KL divergence coefficient β of 0.04.

Baselines. To demonstrate the effectiveness of MedAD-R1, we conduct a comprehensive comparison against a suite of SOTA models. Our baselines are organized into two categories: (1) **Domain-Specific Medical LMMs** (marked with *): HuatuoGPT-Vision [Chen *et al.*, 2024], Lingshu [Xu *et al.*, 2025], LLaVA-Med [Li *et al.*, 2023], and MedVLM [Pan *et al.*, 2025]; and (2) **General-Purpose LMMs**. The latter category encompasses a wide array of leading models to test for broad capabilities, including models from the Qwen family (Qwen2.5-VL-3B, 7B, and 72B versions) [Bai *et al.*, 2025] and the InternVL family (InternVL3.5-8B and 38B versions) [Zhu *et al.*, 2025]. We also include MiMo-VL-7B [Xiaomi *et al.*, 2025], MiniCPM-V-4.5-9B [Yu *et al.*, 2025], GLM-4.1V-Thinking [Hong *et al.*, 2025], Llama3.2-11B-Vision [Grattafiori *et al.*, 2024], ERNIE-4.5-VL-28B [Baidu-ERNIE-Team, 2025], Qwen3VL-32B, and Grok4-Fast. This diverse selection allows for a rigorous evaluation across a

broad spectrum of model scales (from 3B to 72B+ parameters) and architectures. To ensure statistical robustness, all reported performance metrics are the average of three independent runs with different random seeds, and we report both the mean and the standard deviation (std) for all results.

4.2 Comparison with SOTA Models

The main comparison results on the MedAD-38K benchmark are presented in Table 1. The results provide compelling evidence of MedAD-R1’s superiority. It not only achieves the highest Overall Accuracy of 85.15%, surpassing the strongest baseline (Grok4-Fast) by a remarkable 8.15% absolute margin, but also consistently outperforms all other models across every individual task. Notably, MedAD-R1 surpasses even domain-specific models like HuatuoGPT-Vision by nearly 10%, suggesting that current medical LMMs trained with standard SFT are still failing to capture the deep reasoning required for this task. This comprehensive dominance highlights the profound effectiveness of our two-stage training paradigm and the Con-GRPO algorithm in cultivating robust diagnostic and reasoning capabilities.

Further analysis indicates that MedAD-R1’s most significant advantages lie in the most cognitively demanding tasks. For instance, in *Anomaly Detection* and *Lesion Localization*, our model achieves absolute gains of 18.3% and 18.44% respectively, over the best-performing baseline in each category. In contrast, most baselines exhibit limited proficiency on these tasks, often struggling to surpass 60% in detection and 40% in localization, indicating a systemic weakness in their reasoning abilities. represents a substantial leap in capability on these fronts. This disparity strongly validates our central hypothesis: explicit reasoning reinforcement is essential for achieving expert-level performance in medical AI.

Furthermore, MedAD-R1’s SOTA performance is a remarkable achievement for a 3B parameter model, underscoring its exceptional efficiency. A direct comparison with the Qwen2.5VL-3B baseline, which uses the same backbone, shows an substantial 13.74% improvement, directly attributing this gain to our framework rather than the base model’s scale. It decisively outperforms models up to 24 \times its size, such as the 72B Qwen2.5VL, not just in overall accuracy but particularly in reasoning-intensive tasks. This indicates that our proposed Con-GRPO algorithm provides a more stable and effective training signal, allowing a much smaller model to learn complex diagnostic pathways more efficiently than larger models trained with conventional methods. These results validate that our lightweight yet powerful MedAD-R1 framework achieves an optimal balance of accuracy and efficiency, enhancing its feasibility for deployment in real-world clinical settings with limited computational resources.

4.3 Ablation Study

To dissect the contribution of each component within our framework and validate our design choices, we conduct a series of ablation studies. The results are summarized in Table 2 and Table 3.

First, we validate the necessity of our two-stage training paradigm, as shown in Table 2. The RL-only model, trained without the benefit of the SFT stage, performs poorly, with

Table 1: Main results on the MedAD-38K test set. All models are evaluated based on Accuracy (%) for five tasks. The best performance is in **bold**, and the second best is underlined. * indicates domain-specific medical LMMs.

| Model | Params | Anatomy ID. | Anomaly Det. | Lesion Loc. | Modality Class. | Pathology Char. | Overall |
|------------------------|-----------|----------------------------------|----------------------------------|----------------------------------|----------------------------------|----------------------------------|----------------------------------|
| Qwen2.5-VL-3B | 3B | 93.20 \pm 0.34 | 51.27 \pm 0.74 | 24.57 \pm 6.82 | 91.78 \pm 0.39 | 65.30 \pm 1.94 | 71.41 \pm 1.19 |
| Qwen2.5-VL-7B | 7B | 83.98 \pm 3.46 | 55.71 \pm 3.35 | 35.62 \pm 1.88 | 88.45 \pm 2.39 | 48.90 \pm 6.78 | 70.48 \pm 1.23 |
| MiMo-VL-RL | 7B | 88.43 \pm 0.43 | 57.35 \pm 0.54 | 32.98 \pm 1.62 | 90.40 \pm 2.88 | 50.37 \pm 8.88 | 72.44 \pm 0.88 |
| InternVL3.5 | 8B | 94.02 \pm 3.88 | 59.27 \pm 2.05 | 27.84 \pm 2.42 | 92.19 \pm 3.88 | 58.58 \pm 5.29 | 74.46 \pm 3.13 |
| MiniCPM-V-4.5 | 9B | 91.16 \pm 1.70 | 56.43 \pm 1.18 | 16.31 \pm 2.28 | 92.95 \pm 2.47 | 54.60 \pm 2.85 | 71.48 \pm 1.22 |
| GLM-4.1V-Thinking | 9B | 94.87 \pm 1.55 | 52.05 \pm 2.24 | 27.60 \pm 1.45 | 96.59 \pm 1.99 | 58.78 \pm 3.28 | 74.02 \pm 3.96 |
| Llama-3.2-Vision | 11B | 92.38 \pm 1.16 | 47.29 \pm 1.74 | 22.22 \pm 2.38 | 95.21 \pm 1.91 | 50.33 \pm 2.15 | 70.59 \pm 1.14 |
| ERNIE-4.5-VL | 28B | 90.49 \pm 1.95 | 48.66 \pm 1.38 | 24.19 \pm 1.27 | 91.68 \pm 2.45 | 52.13 \pm 2.07 | 69.73 \pm 0.60 |
| Qwen3VL | 32B | 94.68 \pm 0.58 | 56.67 \pm 3.19 | 32.80 \pm 0.61 | 95.29 \pm 0.62 | 54.60 \pm 1.07 | 75.44 \pm 0.62 |
| InternVL3.5 | 38B | 93.39 \pm 2.68 | 58.30 \pm 4.46 | 31.57 \pm 1.02 | 94.25 \pm 2.56 | 71.52 \pm 1.76 | 75.16 \pm 2.45 |
| Qwen2.5VL-72B | 72B | 93.75 \pm 1.16 | 59.24 \pm 1.52 | 37.46 \pm 2.41 | 94.32 \pm 1.43 | 53.43 \pm 1.39 | 76.25 \pm 1.45 |
| Grok4-Fast | / | 93.47 \pm 0.61 | 59.94 \pm 1.56 | 24.90 \pm 1.27 | 92.09 \pm 2.38 | 39.49 \pm 1.05 | 77.00 \pm 1.00 |
| HuatuoGPT-Vision* | 7B | 95.65 \pm 0.36 | 55.78 \pm 1.38 | 33.79 \pm 4.23 | 95.08 \pm 0.16 | 59.58 \pm 1.76 | 75.56 \pm 0.51 |
| Lingshu* | 7B | 96.18 \pm 0.37 | 59.57 \pm 0.82 | 31.75 \pm 2.45 | 76.00 \pm 4.65 | 32.09 \pm 6.24 | 70.91 \pm 1.60 |
| LLaVA-Med* | 7B | <u>86.45\pm7.52</u> | 45.82 \pm 4.36 | 20.81 \pm 4.36 | 81.63 \pm 10.74 | 39.55 \pm 9.78 | 64.36 \pm 3.53 |
| MedVLM* | 2B | 91.17 \pm 0.59 | 48.13 \pm 1.17 | 30.37 \pm 6.09 | 93.45 \pm 0.34 | 74.63 \pm 2.24 | 71.23 \pm 0.53 |
| MedAD-R1 (Ours) | 3B | 98.87\pm0.35 | 78.24\pm0.84 | 55.90\pm1.02 | 97.14\pm0.76 | 79.49\pm1.20 | 85.15\pm0.95 |

its accuracy collapsing to 73.22%. This result confirms our hypothesis that starting reinforcement learning from an unaligned, generalist policy is ineffective. In contrast, the SFT-only model achieves a strong baseline accuracy of 75.41%, demonstrating that the SFT stage provides an essential “cognitive injection.” This step establishes a high-quality initial policy, making the subsequent reinforcement learning problem tractable and efficient.

Table 2: Ablation study of different model components on the MedAD-38K testset. Results are mean Overall Accuracy (%) \pm std.

| Model Configuration | Overall Accuracy (%) |
|------------------------------|------------------------------------|
| RL-only (Con-GRPO) | 73.22 \pm 2.58 |
| SFT-only | 75.41 \pm 1.19 |
| SFT + GRPO (Acc-only) | 78.85 \pm 1.08 |
| SFT + GRPO (Con-only) | 81.73 \pm 1.12 |
| MedAD-R1 (Full Model) | 85.15 \pm 0.95 |

Next, we analyze the critical role of our consistency reward within the reinforcement learning stage. Implementing RL with only a conventional accuracy reward (SFT + GRPO (Acc-only)) lifts performance to 78.85%. While this demonstrates a clear benefit of policy optimization, it still permits the model to learn shortcuts, such as relying on spurious correlations to reach correct answers, and thus fails to address the core issue of clinical trustworthiness. The most striking finding comes from the SFT + GRPO (Con-only) variant. By rewarding the model solely for the logical coherence between its thought and answer, it achieves an even higher accuracy of 81.73%. This provides powerful evidence that rewarding a correct *process* is a more effective learning signal than merely rewarding a correct *outcome*, as it forces the model to learn a more robust and causal understanding of the diagnostic task.

Finally, we justify our choice of a balanced reward function. The results in Table 3 empirically validate our design, showing that the balanced setting achieves the best performance. This confirms our hypothesis that structural format, accuracy, and consistency are all critical and synergistic components. Interestingly, the Consistency-focused setting yields the second-best result (84.21%), significantly

outperforming the Accuracy-focused setting (82.54%). This further reinforces our central claim that enforcing a logically coherent reasoning process is the most potent signal for guiding the model towards a robust and generalizable solution for MedAD. The full MedAD-R1 model, with its balanced reward, effectively leverages this consistency as a structural regularizer while using the accuracy reward to fine-tune the reasoning towards the clinically correct conclusion, ultimately achieving state-of-the-art performance.

Table 3: Ablation of reward weights in the Con-GRPO algorithm.

| Configuration | λ_{fmt} | λ_{acc} | λ_{con} | Accuracy (%) |
|------------------------|------------------------|------------------------|------------------------|------------------------------------|
| Format-focused | 0.8 | 0.1 | 0.1 | 77.13 \pm 1.35 |
| Accuracy-focused | 0.1 | 0.8 | 0.1 | 82.54 \pm 1.02 |
| Consistency-focused | 0.1 | 0.1 | 0.8 | 84.21 \pm 0.98 |
| Balanced (Ours) | 1/3 | 1/3 | 1/3 | 85.15 \pm 0.95 |

5 Conclusion

In this work, we address the dual challenges of data fragmentation and the superficial reasoning induced by standard SFT in MedAD. We construct MedAD-38K, the first large-scale, multi-modal, and multi-center benchmark specifically equipped with detailed CoT annotations to foster reasoning-driven models. Building on this foundation, we propose a novel two-stage training framework that integrates essential knowledge injection via SFT with deep reasoning reinforcement using our Con-GRPO algorithm. At its core, Con-GRPO employs a unique consistency reward that enables the model to transcend superficial correlations, compelling its diagnostic process to be logically coherent with the final conclusion. Our method, MedAD-R1, establishes a new performance standard on this benchmark with a lightweight 3B architecture. This combination of high performance and efficiency is crucial for practical clinical adoption. More importantly, it produces the transparent and internally consistent reasoning pathways that are a prerequisite for clinical trust, paving the way for AI systems that function as trustworthy and collaborative partners in clinical practice.

References

[Achiam *et al.*, 2023] Josh Achiam, Steven Adler, Sandhini Agarwal, Lama Ahmad, Ilge Akkaya, Florencia Leoni Aleman, Diogo Almeida, Janko Altenschmidt, Sam Altman, Shyamal Anadkat, et al. Gpt-4 technical report. *arXiv preprint arXiv:2303.08774*, 2023.

[Al-Dhabyani *et al.*, 2020] Walid Al-Dhabyani, Mohammed Gomaa, Hussien Khaled, and Aly Fahmy. Dataset of breast ultrasound images. *Data in brief*, 28:104863, 2020.

[Alsaheel *et al.*, 2021] Abdulellah Alsaheel, Yuhong Nan, Shiqing Ma, Le Yu, Gregory Walkup, Z Berkay Celik, Xiangyu Zhang, and Dongyan Xu. {ATLAS}: A sequence-based learning approach for attack investigation. In *30th USENIX security symposium (USENIX security 21)*, pages 3005–3022, 2021.

[Aresta *et al.*, 2019] Guilherme Aresta, Teresa Araújo, Scotty Kwok, Sai Saketh Chennamsetty, Mohammed Safwan, Varghese Alex, Bahram Marami, Marcel Prastawa, Monica Chan, Michael Donovan, et al. Bach: Grand challenge on breast cancer histology images. *Medical image analysis*, 56:122–139, 2019.

[Bai *et al.*, 2025] Shuai Bai, Keqin Chen, Xuejing Liu, Jialin Wang, Wenbin Ge, Sibo Song, Kai Dang, Peng Wang, Shijie Wang, Jun Tang, et al. Qwen2. 5-vl technical report. *arXiv preprint arXiv:2502.13923*, 2025.

[Baid *et al.*, 2021] Ujjwal Baid, Satyam Ghodasara, Suyash Mohan, Michel Bilello, Evan Calabrese, Errol Colak, Keyvan Farahani, Jayashree Kalpathy-Cramer, Felipe C Kitamura, Sarthak Pati, et al. The rsna-asnr-miccai brats 2021 benchmark on brain tumor segmentation and radiogenomic classification. *arXiv preprint arXiv:2107.02314*, 2021.

[Baidu-ERNIE-Team, 2025] Baidu-ERNIE-Team. Ernie 4.5 technical report, 2025.

[Bernal *et al.*, 2015] Jorge Bernal, F Javier Sánchez, Gloria Fernández-Esparrach, Debora Gil, Cristina Rodríguez, and Fernando Vilaríño. Wm-dova maps for accurate polyp highlighting in colonoscopy: Validation vs. saliency maps from physicians. *Computerized medical imaging and graphics*, 43:99–111, 2015.

[Bilic *et al.*, 2023] Patrick Bilic, Patrick Christ, Hong-wei Bran Li, Eugene Vorontsov, Avi Ben-Cohen, Georgios Kaassis, Adi Szeskin, Colin Jacobs, Gabriel Efrain Hum-pire Mamani, Gabriel Chartrand, et al. The liver tumor segmentation benchmark (lits). *Medical image analysis*, 84:102680, 2023.

[Cai *et al.*, 2024] Yu Cai, Hao Chen, and Kwang-Ting Cheng. Rethinking autoencoders for medical anomaly detection from a theoretical perspective. In *International Conference on Medical Image Computing and Computer-Assisted Intervention*, pages 544–554. Springer, 2024.

[Chen *et al.*, 2024] Junying Chen, Chi Gui, Ruyi Ouyang, Anningzhe Gao, Shunian Chen, Guiming Hardy Chen, Xidong Wang, Ruifei Zhang, Zhenyang Cai, Ke Ji, et al. Huatuogpt-vision, towards injecting medical visual knowledge into multimodal llms at scale. *arXiv preprint arXiv:2406.19280*, 2024.

[Codella *et al.*, 2019] Noel Codella, Veronica Rotemberg, Philipp Tschandl, M Emre Celebi, Stephen Dusza, David Gutman, Brian Helba, Aadi Kalloo, Konstantinos Liopyris, Michael Marchetti, et al. Skin lesion analysis toward melanoma detection 2018: A challenge hosted by the international skin imaging collaboration (isic). *arXiv preprint arXiv:1902.03368*, 2019.

[Comanici *et al.*, 2025] Gheorghe Comanici, Eric Bieber, Mike Schaekermann, Ice Pasupat, Noveen Sachdeva, Inderjit Dhillon, Marcel Blistein, Ori Ram, Dan Zhang, Evan Rosen, et al. Gemini 2.5: Pushing the frontier with advanced reasoning, multimodality, long context, and next generation agentic capabilities. *arXiv preprint arXiv:2507.06261*, 2025.

[Grattafiori *et al.*, 2024] Aaron Grattafiori, Abhimanyu Dubey, Abhinav Jauhri, Abhinav Pandey, Abhishek Kadian, Ahmad Al-Dahle, Aiesha Letman, Akhil Mathur, Alan Schelten, Alex Vaughan, et al. The llama 3 herd of models. *arXiv preprint arXiv:2407.21783*, 2024.

[Gudibande *et al.*, 2023] Arnav Gudibande, Eric Wallace, Charlie Snell, Xinyang Geng, Hao Liu, Pieter Abbeel, Sergey Levine, and Dawn Song. The false promise of imitating proprietary llms. *arXiv preprint arXiv:2305.15717*, 2023.

[Hamada, 2020] Ahmed Hamada. Br35h :: Brain tumor detection 2020. IEEE DataPort, 2020.

[Hong *et al.*, 2025] Wenyi Hong, Wenmeng Yu, Xiaotao Gu, Guo Wang, Guobing Gan, Haomiao Tang, Jiale Cheng, Ji Qi, Junhui Ji, Lihang Pan, et al. Glm-4.1 v-thinking: Towards versatile multimodal reasoning with scalable reinforcement learning. *arXiv preprint arXiv:2507.01006*, 2025.

[Hu *et al.*, 2019] Junjie Hu, Yuanyuan Chen, and Zhang Yi. Automated segmentation of macular edema in oct using deep neural networks. *Medical image analysis*, 55:216–227, 2019.

[Iqbal *et al.*, 2023] Hasan Iqbal, Umar Khalid, Chen Chen, and Jing Hua. Unsupervised anomaly detection in medical images using masked diffusion model. In *International Workshop on Machine Learning in Medical Imaging*, pages 372–381. Springer, 2023.

[Jha *et al.*, 2019] Debesh Jha, Pia H Smedsrød, Michael A Riegler, Pål Halvorsen, Thomas De Lange, Dag Johansen, and Håvard D Johansen. Kvasir-seg: A segmented polyp dataset. In *International conference on multimedia modeling*, pages 451–462. Springer, 2019.

[Kingma and Ba, 2014] Diederik P Kingma and Jimmy Ba. Adam: A method for stochastic optimization. *arXiv preprint arXiv:1412.6980*, 2014.

[Li *et al.*, 2023] Chunyuan Li, Cliff Wong, Sheng Zhang, Naoto Usuyama, Haotian Liu, Jianwei Yang, Tristan

Naumann, Hoifung Poon, and Jianfeng Gao. Llamed: Training a large language-and-vision assistant for biomedicine in one day. *Advances in Neural Information Processing Systems*, 36:28541–28564, 2023.

[Mendonça *et al.*, 2013] Teresa Mendonça, Pedro M Ferreira, Jorge S Marques, André RS Marcal, and Jorge Rozeira. Ph 2-a dermoscopic image database for research and benchmarking. In *2013 35th annual international conference of the IEEE engineering in medicine and biology society (EMBC)*, pages 5437–5440. IEEE, 2013.

[Moor *et al.*, 2023] Michael Moor, Qian Huang, Shirley Wu, Michihiro Yasunaga, Yash Dalmia, Jure Leskovec, Cyril Zakka, Eduardo Pontes Reis, and Pranav Rajpurkar. Medflamingo: a multimodal medical few-shot learner. In *Machine Learning for Health (ML4H)*, pages 353–367. PMLR, 2023.

[Morozov *et al.*, 2020] Sergey P Morozov, Anna E Andreychenko, Ivan A Blokhin, Pavel B Gelezhe, Anna P Gonchar, Alexander E Nikolaev, Nikolay A Pavlov, Valeria Yu Chernina, and Victor A Gombolevskiy. Mosmeddata: data set of 1110 chest ct scans performed during the covid-19 epidemic. *Digital Diagnostics*, 1(1):49–59, 2020.

[Orlov *et al.*, 2010] Nikita V Orlov, Wayne W Chen, David Mark Eckley, Tomasz J Macura, Lior Shamir, Elaine S Jaffe, and Ilya G Goldberg. Automatic classification of lymphoma images with transform-based global features. *IEEE Transactions on Information Technology in Biomedicine*, 14(4):1003–1013, 2010.

[Pan *et al.*, 2025] Jiazen Pan, Che Liu, Junde Wu, Fenglin Liu, Jiayuan Zhu, Hongwei Bran Li, Chen Chen, Cheng Ouyang, and Daniel Rueckert. Medvilm-r1: Incentivizing medical reasoning capability of vision-language models (vlms) via reinforcement learning. In *International Conference on Medical Image Computing and Computer-Assisted Intervention*, pages 337–347. Springer, 2025.

[Pedraza *et al.*, 2015] Lina Pedraza, Carlos Vargas, Fabián Narváez, Oscar Durán, Emma Muñoz, and Eduardo Romero. An open access thyroid ultrasound image database. In *10th International symposium on medical information processing and analysis*, volume 9287, pages 188–193. SPIE, 2015.

[Popa and Visa, 2025] Maria Popa and Gabriela Adriana Visa. Pedidemi—a pediatric demyelinating lesion segmentation dataset. *arXiv preprint arXiv:2508.13239*, 2025.

[Porwal *et al.*, 2018] Prasanna Porwal, Samiksha Pachade, Ravi Kamble, Manesh Kokare, Girish Deshmukh, Vivek Sahasrabuddhe, and Fabrice Meriaudeau. Indian diabetic retinopathy image dataset (idrid): a database for diabetic retinopathy screening research. *Data*, 3(3):25, 2018.

[Prevedello *et al.*, 2019] Luciano M Prevedello, Safwan S Halabi, George Shih, Carol C Wu, Marc D Kohli, Falgun H Chokshi, Bradley J Erickson, Jayashree Kalpathy-Cramer, Katherine P Andriole, and Adam E Flanders. Challenges related to artificial intelligence research in medical imaging and the importance of image analysis competitions. *Radiology: Artificial Intelligence*, 1(1):e180031, 2019.

[Schulman *et al.*, 2017] John Schulman, Filip Wolski, Profulla Dhariwal, Alec Radford, and Oleg Klimov. Proximal policy optimization algorithms. *arXiv preprint arXiv:1707.06347*, 2017.

[Sellergren *et al.*, 2025] Andrew Sellergren, Sahar Kazemzadeh, Tiam Jaroensri, Atilla Kiraly, Madeleine Traverse, Timo Kohlberger, Shawn Xu, Fayaz Jamil, Cian Hughes, Charles Lau, et al. Medgemma technical report. *arXiv preprint arXiv:2507.05201*, 2025.

[Shao *et al.*, 2024] Zhihong Shao, Peiyi Wang, Qihao Zhu, Runxin Xu, Junxiao Song, Xiao Bi, Haowei Zhang, Mingchuan Zhang, YK Li, Y Wu, et al. Deepseekmath: Pushing the limits of mathematical reasoning in open language models. *arXiv preprint arXiv:2402.03300*, 2024.

[Wang *et al.*, 2017] Xiaosong Wang, Yifan Peng, Le Lu, Zhiyong Lu, Mohammadhadi Bagheri, and Ronald M Summers. Chestx-ray8: Hospital-scale chest x-ray database and benchmarks on weakly-supervised classification and localization of common thorax diseases. In *Proceedings of the IEEE conference on computer vision and pattern recognition*, pages 2097–2106, 2017.

[Xiaomi *et al.*, 2025] LLM Xiaomi, Bingquan Xia, Bowen Shen, Dawei Zhu, Di Zhang, Gang Wang, Hailin Zhang, Huaiqiu Liu, Jiebao Xiao, Jinhao Dong, et al. Mimo: Unlocking the reasoning potential of language model—from pretraining to posttraining. *arXiv preprint arXiv:2505.07608*, 2025.

[Xu *et al.*, 2025] Weiwen Xu, Hou Pong Chan, Long Li, Mahani Aljunied, Ruijing Yuan, Jianyu Wang, Chenghao Xiao, Guizhen Chen, Chaoqun Liu, Zhaodonghui Li, et al. Lingshu: A generalist foundation model for unified multimodal medical understanding and reasoning. *arXiv preprint arXiv:2506.07044*, 2025.

[Yu *et al.*, 2025] Tianyu Yu, Zefan Wang, Chongyi Wang, Fuwei Huang, Wenshuo Ma, Zhihui He, Tianchi Cai, Weize Chen, Yuxiang Huang, Yuanqian Zhao, et al. Minicpm-v 4.5: Cooking efficient mllms via architecture, data, and training recipe. *arXiv preprint arXiv:2509.18154*, 2025.

[Zhang *et al.*, 2023] Zhuosheng Zhang, Aston Zhang, Mu Li, Hai Zhao, George Karypis, and Alex Smola. Multimodal chain-of-thought reasoning in language models. *arXiv preprint arXiv:2302.00923*, 2023.

[Zhang *et al.*, 2024] Ximiao Zhang, Min Xu, Dehui Qiu, Ruixin Yan, Ning Lang, and Xiuzhuang Zhou. Mediclip: Adapting clip for few-shot medical image anomaly detection. In *International Conference on Medical Image Computing and Computer-Assisted Intervention*, pages 458–468. Springer, 2024.

[Zhu *et al.*, 2025] Jinguo Zhu, Weiyun Wang, Zhe Chen, Zhaoyang Liu, Shenglong Ye, Lixin Gu, Hao Tian, Yuchen Duan, Weijie Su, Jie Shao, et al. Internvl3: Exploring advanced training and test-time recipes for open-source multimodal models. *arXiv preprint arXiv:2504.10479*, 2025.